

## Diene–Metal $\pi$ Bonding. Some Unexpected Effects of Group 5 Donor Ligands on Carbon-13 Nuclear Magnetic Resonance Parameters and X-Ray Crystal Structures

By Anthony J. Pearson\* and Paul R. Raithby, University Chemical Laboratory, Lensfield Road, Cambridge CB2 1EW

A number of  $\eta^4$ -cyclohexadiene–Fe(CO)<sub>2</sub>L and  $\eta^4$ -2-methoxycyclohexadiene–Fe(CO)<sub>2</sub>L complexes have been prepared and their <sup>13</sup>C n.m.r. spectra recorded. Methoxy-substituent effects suggest a depopulation rather than the expected enhanced population of the diene l.u.m.o. (lowest unoccupied molecular orbital) as the  $\pi$ -acceptor strength of L decreases. X-Ray crystal-structure determinations for L = PPh<sub>3</sub> were in agreement, and an explanation is proposed. Complexes [Fe(CO)<sub>2</sub>(PPh<sub>3</sub>)(C<sub>6</sub>H<sub>8</sub>)] (7) and [Fe(CO)<sub>2</sub>(PPh<sub>3</sub>)(C<sub>6</sub>H<sub>7</sub>OMe)] (8) both crystallise in the monoclinic space group *P*2<sub>1</sub>/*c* with *Z* = 4. The cell parameters are *a* = 10.289(4), *b* = 24.651(10), *c* = 9.282(4) Å, and  $\beta$  = 109.37(3)° for (7) and *a* = 14.444(7), *b* = 18.052(10), *c* = 9.229(4) Å, and  $\beta$  = 100.57(4)° for (8). The structures were solved by a combination of Patterson and Fourier-difference techniques, and refined by blocked-cascade least squares to *R* = 0.053 for 3 325 unique observed reflections (7) and to *R* = 0.062 for 2 952 reflections (8).

MOLECULAR-ORBITAL calculations can only be considered as valid approximations when their predictions are verified experimentally. In this respect, the Hückel approximation applied to conjugated systems, and the subsequent development of Frontier Orbital treatments, have proved to be an exceptionally useful aid in predicting the outcome of a large number of pericyclic reactions.<sup>1</sup> With regard to bonding in metal–olefin  $\pi$  complexes, a number of treatments have evolved from the basic Chatt–Dewar–Duncanson concept.<sup>2</sup> In particular, the bonding between a transition metal and a conjugated diene, exemplified by the well known tricarbonyl(diene)iron complexes, has been treated at a number of levels, from the simple text-book description<sup>3</sup> to more sophisticated molecular-orbital calculations.<sup>4–6</sup> All of these treatments tell us that there is a donation of electrons from the highest occupied molecular orbital (h.o.m.o.) of the diene to vacant metal *d* orbitals (or hybrid orbitals), accompanied by a back donation from a filled metal orbital into the diene lowest unoccupied molecular orbital (l.u.m.o.). This should result in a decrease in  $\pi$ -bond order for the terminal diene C–C bond and an increase for the central C–C bond, compared to the uncomplexed diene, and this is confirmed by the growing amount of X-ray crystal-structure data, where it is found that the central bond is slightly shorter than the terminal bonds,<sup>7</sup> whilst electron diffraction studies on uncomplexed butadiene reveal the terminal bonds to be shorter (1.34 Å) than the central bond (1.48 Å).<sup>8</sup> However, X-ray diffraction is a rather limited technique since small variations in bond lengths can occur due to crystal packing effects, so that it is very difficult to reliably determine small changes in bond orders arising from perturbations of the metal complex m.o.s.<sup>3</sup> Consequently, we recently undertook a study of the effects of substituents on the diene carbon-13 n.m.r. shieldings, based on literature precedent for purely organic systems.<sup>9</sup>

We found that introduction of a substituent at C(2) of the uncomplexed diene caused changes in shielding at C(1) and C(3) ( $\beta$  effects) consistent with the higher  $\pi$ -bond

order in the 1,2- than in the 2,3-bond, whilst the same diene substituent on a diene–Fe(CO)<sub>3</sub> complex gave  $\beta$  effects consistent with the  $\pi$ -bond order now being higher for the central (2,3) bond.<sup>10,11</sup> Moreover, when a 2-methoxy-substituent was employed,<sup>11</sup> the individual effects were very large, and considerably different for complexes and uncomplexed dienes. Thus it occurred to us that the study of <sup>13</sup>C n.m.r. methoxy-substituent effects might be an extremely sensitive way of measuring changes in  $\pi$ -bond orders resulting from small electronic perturbations at the metal.

Such an effect is expected to arise from replacing one or more carbonyl ligands by a weaker (or stronger)  $\pi$  acceptor. It is commonly accepted that substitution with a weaker  $\pi$  acceptor will lead to expansion of the metal *d* orbitals and an increased back donation into the diene l.u.m.o., as is observed and experimentally verified for simple metal carbonyl complexes<sup>12</sup> (where increased back donation into the CO antibonding orbital leads to a lowering of the i.r. stretching frequency). In their review, Churchill and Mason<sup>13</sup> presented crystallographic data supporting this argument, but unfortunately the comparison was made using diene complexes of different metals, so that the changes in bond lengths observed might well be a function of the metal rather than the ligands employed. Consequently, we sought to utilise the n.m.r. method, and where possible X-ray data, for a series of diene–Fe(CO)<sub>2</sub>L complexes in order to further verify the above prediction. Our results are contrary to expectation and indicate a deficiency in current qualitative bonding descriptions. Consequently, we have developed a simple pictorial model which might now be subjected to theoretical treatment and further experimental testing.

### RESULTS AND DISCUSSION

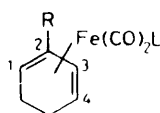
*Infrared Spectra.*—A total of eight complexes (1)–(8) were available for comparison of i.r. spectra. The complexes reported are those which we have been able to obtain in a sufficiently pure state for unambiguous

TABLE 1  
Carbonyl stretching frequencies for diene-Fe(CO)<sub>2</sub>L complexes \*

Complex	$[\nu_{\max.}/\text{cm}^{-1}]$
(1) [Fe(CO) <sub>2</sub> (C <sub>6</sub> H <sub>8</sub> )]	2 060, 1 960
(2) [Fe(CO) <sub>2</sub> (C <sub>6</sub> H <sub>7</sub> OMe)]	2 057, 1 965
(3) [Fe(CO) <sub>2</sub> {P(OMe) <sub>3</sub> }(C <sub>6</sub> H <sub>8</sub> )]	1 983, 1 920
(4) [Fe(CO) <sub>2</sub> {P(OMe) <sub>3</sub> }(C <sub>6</sub> H <sub>7</sub> OMe)]	1 983, 1 920
(5) [Fe(CO) <sub>2</sub> (AsPh <sub>3</sub> )(C <sub>6</sub> H <sub>8</sub> )]	1 970, 1 912
(6) [Fe(CO) <sub>2</sub> (AsPh <sub>3</sub> )(C <sub>6</sub> H <sub>7</sub> OMe)]	1 970, 1 910
(7) [Fe(CO) <sub>2</sub> (PPh <sub>3</sub> )(C <sub>6</sub> H <sub>8</sub> )]	1 970, 1 910
(8) [Fe(CO) <sub>2</sub> (PPh <sub>3</sub> )(C <sub>6</sub> H <sub>7</sub> OMe)]	1 970, 1 908

\* Solutions in chloroform.

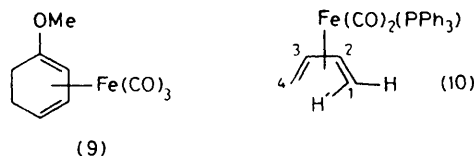
spectral assignments. Incorporation of other ligands for study was desirable but we were limited by the stability and purity of the resultant complexes. Those described here provide sufficient data for the present discussion. The metal carbonyl bands (Table 1) show the expected shift to lower wavenumber as L becomes a weaker  $\pi$  acceptor, as expected, assuming  $\pi$ -acceptor strength varies  $\text{CO} > \text{P(OMe)}_3 > \text{AsPh}_3 \sim \text{PPh}_3$ .<sup>12</sup>



- (1) R = H, L = CO
- (2) R = OMe, L = CO
- (3) R = H, L = P(OMe)<sub>3</sub>
- (4) R = OMe, L = P(OMe)<sub>3</sub>
- (5) R = H, L = AsPh<sub>3</sub>
- (6) R = OMe, L = AsPh<sub>3</sub>
- (7) R = H, L = PPh<sub>3</sub>
- (8) R = OMe, L = PPh<sub>3</sub>

In routinely measuring i.r. spectra of methoxy-substituted cyclohexadiene-Fe(CO)<sub>3</sub> complexes we have observed a consistent and extremely useful difference (for purposes of structure elucidation) between 2-methoxycyclohexadiene and 1-methoxycyclohexadiene complexes, *e.g.* (2) and (9), respectively. Thus, (2) shows a unique strong absorption at 1 485 cm<sup>-1</sup> which is absent in both (1) and (9), these giving only weak absorptions at 1 475–1 400 cm<sup>-1</sup>. It is also not found for the free

ligand from (2). Bands in this region have been previously assigned to stretching of the complexed C=C double bond, the low frequency being attributed to its low  $\pi$ -bond order.<sup>14</sup> Uncomplexed vinyl ethers, including 2-methoxycyclohexa-1,3-dienes and 1-methoxycyclohexa-1,3-dienes, all show a characteristic strong absorption at higher frequency, 1 660–1 690 cm<sup>-1</sup>, than the unsubstituted olefins.<sup>15</sup> We have therefore assigned the unique band in (2) to a co-ordinated vinyl ether group, which must therefore arise from the 2,3-bond, since it is absent in (9). This supports the notion of back donation into the diene l.u.m.o. leading to higher  $\pi$ -bond order in



the 2,3-bond, and is in agreement with our earlier <sup>13</sup>C n.m.r. studies. Unfortunately, the phosphine and arsine ligands used in this study also show absorption around 1 490 cm<sup>-1</sup>, so we were unable to extract useful information from the spectra of complexes (4), (6), and (8).

**Nuclear Magnetic Resonance Spectra.—General features.** Details of proton n.m.r. spectra are given in the Experimental section. Long-range <sup>31</sup>P-<sup>1</sup>H couplings were determined by proton and phosphorus decoupling experiments. Table 2 summarises the <sup>13</sup>C n.m.r. data for complexes (1)–(8). In general, the carbonyl shieldings shift to lower field as L decreases in  $\pi$ -acceptor strength, in complete agreement with the literature for other complexes,<sup>16</sup> whilst the diene carbon resonances shift to higher field by a *small* amount, indicating a small increase in electron density either at the metal or in the diene  $\pi$  orbitals. These data do not differentiate these alternatives, nor indicate whether the diene l.u.m.o. is being further populated. The triphenylphosphine complexes are slightly out of line, since we should expect the shifts to be similar to those for triphenylarsine (see later).

TABLE 2  
Carbon-13 n.m.r. data for diene-Fe(CO)<sub>2</sub>L complexes <sup>a</sup>

Complex	CO	MeO <i>etc.</i>	C(1)	C(2)	C(3)	C(4)	C(5)	C(6)
(1) <sup>b</sup>	212.2		62.5	85.5	85.5	62.5	24.5	
(2) <sup>b</sup>	210.0	54.0	55.1	139.9	67.7	50.9	24.0	25.1
(3)	216.9 (21.5)	51.3 [145]	60.0 (3.9)	83.9 [168.0]	83.9	60.0	24.3 [130]	
(4)	214.1 (20)	51.3 P(OMe) <sub>3</sub> 54.2 OMe	50.3 [154.3]	138.2	68.3	49.7 (5.9)	23.8 (5.9)	25.5
(5)	218.9		59.1 [158.2]	84.0 [168.0]	84.0	59.1	24.5 [134.8]	
(6)	216.1	54.3	49.2	138.3	69.7	48.3	23.6	25.6
(7)	219.1 (13.7)		61.0 (3.7)	84.6 [168.0]	84.6	61.0	24.7 [128.9]	
(8)	216	54.2 [144.5]	52.0 (6.0)	138.4	72.1 [168]	48.0 (9.8)	23.6 (3.9)	25.8 [130]
(11) <sup>b</sup>	211		40.4 [155.3]	85.2	85.2	40.4	24.5 [130]	
(10)	217.7 (13.7)		40.8 [157.2]	84.3 [158]	84.3	40.8		

<sup>a</sup> Shieldings in p.p.m. downfield from SiMe<sub>4</sub>. Spin-spin couplings, ( $J_F$ ) and [ $J_{C,H}$ ], in Hz. <sup>b</sup> Data from refs. 10 and 11.

We also observe small spin-spin couplings between C(1), C(4) and phosphorus for complexes (3), (4), (7), and (8), whilst the central diene carbon atoms, C(2) and C(3), show no coupling. Neither the butadiene complex (10) nor the analogous cycloheptadiene-Fe(CO)<sub>2</sub>(PPh<sub>3</sub>) complex<sup>17</sup> show any coupling between phosphorus and diene carbon atoms. It therefore seems un-

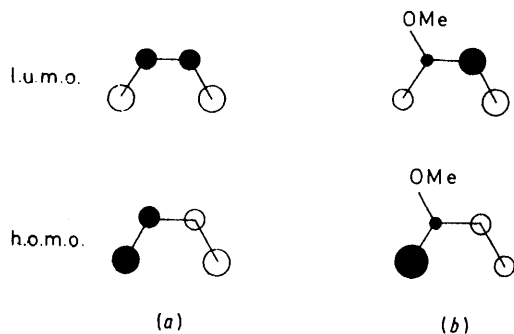


FIGURE 1 H.o.m.o. and l.u.m.o. coefficients for butadiene (a) and 2-methoxybutadiene (b)

likely that this coupling arises from interaction of orbital electronic currents with the nuclear magnetic moments<sup>18</sup> which might have been expected for molecules where *s*, *p*, and *d* orbitals are involved in bonding. It is more likely that the effect is due to a non-zero contact term, so that in the six-membered ring complexes there appears to be a small amount of *s* character at the terminal carbon atoms. That this is absent in the acyclic and larger ring complexes indicates that the constraint on the diene due to ring size induces a slight rehybridisation at the terminal carbons, which is reflected in the n.m.r. spectrum. This is interesting since it indicates in general that bonding of the diene to iron involves pure *p* orbitals, and that wherever rehybridisation occurs it can probably be detected.

We now turn our attention to the methoxy-substituent effects. The available literature<sup>9</sup> suggests that transmission of <sup>13</sup>C n.m.r. substituent effects through unsaturated systems is linearly related to the  $\pi$ -bond orders of the bonds involved. We previously used this fact to show that the central C-C bond in diene-Fe(CO)<sub>3</sub> complexes has greater  $\pi$ -bond order than the terminal bonds.<sup>10,11</sup> We now present a rationalisation of this earlier data based on a simple Frontier Molecular Orbital (f.m.o.) treatment which is important for understanding the effects observed in the present work. The h.o.m.o. and l.u.m.o. coefficients for all-*cis*-butadiene and 2-methoxybutadiene are shown in Figure 1 as Houk diagrams (not to scale).<sup>1,19</sup> The change in h.o.m.o. coefficients between these two are reflected in the <sup>13</sup>C n.m.r. substituent effects. Thus, a 2-methoxy-substituent on the *free* diene leads to a large upfield shift of C(1) ( $\beta_{1,2}$ ), a small upfield shift of C(3) ( $\beta_{2,3}$ ), and a small upfield shift of C(4) ( $\gamma$ ). With diene-Fe(CO)<sub>3</sub> complexes the n.m.r. effects reflect the changes in relative l.u.m.o. coefficients: a small upfield shift of C(1), a large upfield shift of C(3), and an appreciable upfield shift of C(4), indicating the well known population of the diene

l.u.m.o.<sup>3-6</sup> On this basis then, we should expect that any perturbation of the molecule which corresponds effectively to greater population of the diene l.u.m.o. will lead to an enhancement of these effects, *i.e.* greater  $\beta_{2,3}$  and  $\gamma$  effects but smaller  $\beta_{1,2}$  effect. The appropriate substituent effects are calculated in Table 3. It is clear

TABLE 3

<sup>13</sup>C N.m.r. methoxy-substituent effects for diene-Fe(CO)<sub>2</sub>L complexes \*

Complexes compared	$\beta_{1,2}$ [C(1)]	$\beta_{1,2}$ [C(3)]	$\gamma$ [C(4)]
(2) and (1)	-7.4	-17.8	-11.6
(4) and (3)	-9.7	-15.6	-10.3
(6) and (5)	-9.9	-14.3	-10.8
(8) and (7)	-9.0	-12.5	-13.0

\* Values in p.p.m. Negative values indicate shift to higher field.

that the changes are not as expected. They are in fact completely the reverse. The triphenylphosphine effects are slightly anomalous but still fall within the general trend. Clearly then, a weaker  $\pi$ -acceptor ligand L does not lead to greater population of the diene l.u.m.o. We now consider the available crystal-structure data and our data for complexes (7) and (8).

*Description of the Structures (7) and (8).*—Both molecules exist in the solid state as discrete, neutral monomers separated by normal van der Waals distances. Figure 2 shows the molecular structure of (7) and in-

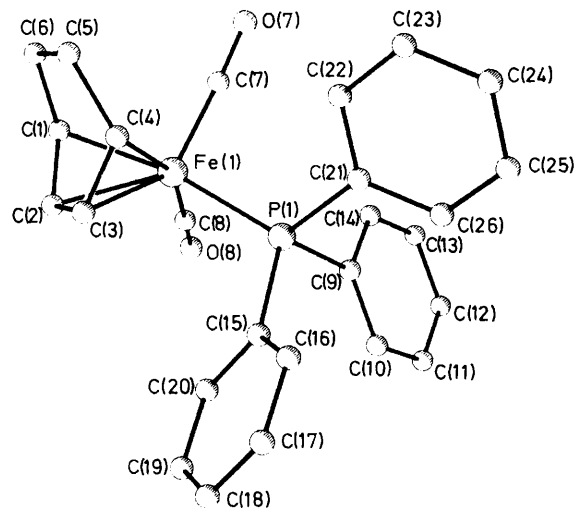


FIGURE 2 The molecular structure of (7)

cludes the atom-numbering scheme adopted; hydrogen atoms have been omitted for clarity. The bond lengths and angles for this structure are given in Tables 4 and 5 respectively. The molecular structure of (8) is illustrated in Figure 3, and the bond parameters associated with this complex are listed in Tables 6 and 7.

The overall molecular geometry of these two complexes closely resembles that of related cyclohexadiene tricarbonyliron species.<sup>20</sup> In (8) the methoxy-group adopts the *exo* stereochemistry. The C(1)C(2)C(3)C(4) diene fragment in the two compounds is planar to

TABLE 4

Bond lengths (Å) for complex (7)

Fe(1)-C(1)	2.101(4)	C(1)-C(2)	1.408(7)
Fe(1)-C(2)	2.051(4)	C(1)-C(6)	1.533(6)
Fe(1)-C(3)	2.057(4)	C(2)-C(3)	1.414(6)
Fe(1)-C(4)	2.111(4)	C(3)-C(4)	1.404(7)
Fe(1)-C(7)	1.752(5)	C(4)-C(5)	1.521(7)
Fe(1)-C(8)	1.770(4)	C(5)-C(6)	1.520(6)
Fe(1)-P(1)	2.232(1)	C(7)-O(7)	1.151(7)
P(1)-C(9)	1.841(3)	C(8)-O(8)	1.142(5)
P(1)-C(15)	1.834(4)	C(9)-C(10)	1.377(6)
P(1)-C(21)	1.840(4)	C(9)-C(14)	1.392(6)
C(15)-C(16)	1.378(6)	C(10)-C(11)	1.397(6)
C(15)-C(20)	1.392(6)	C(11)-C(12)	1.364(8)
C(16)-C(17)	1.404(7)	C(12)-C(13)	1.377(8)
C(17)-C(18)	1.357(7)	C(13)-C(14)	1.391(6)
C(18)-C(19)	1.378(8)	C(21)-C(22)	1.396(6)
C(19)-C(20)	1.378(8)	C(21)-C(26)	1.399(5)
C(22)-C(23)	1.396(6)	C(23)-C(24)	1.376(6)
C(24)-C(25)	1.391(7)	C(25)-C(26)	1.334(6)

TABLE 5

Bond angles (°) for complex (7)

C(1)-Fe(1)-C(2)	39.6(2)	Fe(1)-C(1)-C(2)	68.3(2)
C(1)-Fe(1)-C(3)	69.8(2)	Fe(1)-C(1)-C(6)	109.8(3)
C(2)-Fe(1)-C(3)	40.3(2)	Fe(1)-C(2)-C(1)	72.1(2)
C(1)-Fe(1)-C(4)	76.2(2)	Fe(1)-C(2)-C(3)	70.1(2)
C(2)-Fe(1)-C(4)	69.6(2)	Fe(1)-C(3)-C(2)	69.7(2)
C(3)-Fe(1)-C(4)	39.4(2)	Fe(1)-C(3)-C(4)	72.4(2)
C(1)-Fe(1)-C(7)	92.8(2)	Fe(1)-C(4)-C(3)	68.2(2)
C(2)-Fe(1)-C(7)	131.8(2)	Fe(1)-C(4)-C(5)	109.4(3)
C(3)-Fe(1)-C(7)	134.6(2)	C(2)-C(1)-C(6)	119.8(4)
C(4)-Fe(1)-C(7)	96.7(2)	C(1)-C(2)-C(3)	115.0(4)
C(1)-Fe(1)-C(8)	93.5(2)	C(2)-C(3)-C(4)	114.9(4)
C(2)-Fe(1)-C(8)	91.0(2)	C(3)-C(4)-C(5)	120.5(4)
C(3)-Fe(1)-C(8)	120.4(2)	C(4)-C(5)-C(6)	111.0(4)
C(4)-Fe(1)-C(8)	159.4(2)	C(1)-C(6)-C(5)	110.4(4)
C(7)-Fe(1)-C(8)	101.6(2)	Fe(1)-C(7)-O(7)	177.3(3)
C(1)-Fe(1)-P(1)	166.2(1)	Fe(1)-C(8)-O(8)	178.1(4)
C(2)-Fe(1)-P(1)	127.5(1)	Fe(1)-P(1)-C(9)	114.1(1)
C(3)-Fe(1)-P(1)	96.5(1)	Fe(1)-P(1)-C(15)	115.0(1)
C(4)-Fe(1)-P(1)	94.8(1)	Fe(1)-P(1)-C(21)	118.8(1)
C(7)-Fe(1)-P(1)	98.7(1)	C(9)-P(1)-C(15)	102.9(2)
C(8)-Fe(1)-P(1)	91.7(1)	C(9)-P(1)-C(21)	100.1(2)
P(1)-C(9)-C(10)	124.3(3)	C(15)-P(1)-C(21)	103.8(2)
P(1)-C(9)-C(14)	116.9(3)	P(1)-C(15)-C(16)	124.4(3)
C(10)-C(9)-C(14)	118.8(3)	P(1)-C(15)-C(20)	116.8(3)
C(9)-C(10)-C(11)	120.0(5)	C(16)-C(15)-C(20)	118.7(4)
C(10)-C(11)-C(12)	120.9(5)	C(15)-C(16)-C(17)	119.7(4)
C(11)-C(12)-C(13)	119.8(4)	C(16)-C(17)-C(18)	120.6(4)
C(12)-C(13)-C(14)	119.9(5)	C(17)-C(18)-C(19)	120.3(5)
C(9)-C(14)-C(13)	120.6(4)	C(18)-C(19)-C(20)	119.6(5)
P(1)-C(21)-C(22)	120.5(3)	C(15)-C(20)-C(19)	121.1(4)
P(1)-C(21)-C(26)	121.1(3)	C(22)-C(21)-C(26)	118.4(3)
C(21)-C(22)-C(23)	120.0(4)	C(22)-C(23)-C(24)	120.8(5)
C(23)-C(24)-C(25)	119.5(4)	C(24)-C(25)-C(26)	120.1(4)
C(21)-C(26)-C(25)	121.3(4)		

TABLE 6

Bond lengths (Å) for complex (8)

Fe(1)-C(1)	2.122(5)	C(1)-C(2)	1.408(8)
Fe(1)-C(2)	2.105(6)	C(1)-C(6)	1.505(8)
Fe(1)-C(3)	2.063(5)	C(2)-C(3)	1.410(7)
Fe(1)-C(4)	2.092(5)	C(3)-C(4)	1.426(8)
Fe(1)-P(1)	2.225(1)	C(4)-C(5)	1.519(8)
Fe(1)-C(8)	1.741(6)	C(5)-C(6)	1.538(7)
Fe(1)-C(9)	1.768(5)	C(2)-O(1)	1.367(7)
P(1)-C(101)	1.853(4)	O(1)-C(7)	1.453(9)
P(1)-C(111)	1.843(3)	C(8)-O(2)	1.162(8)
P(1)-C(121)	1.829(3)	C(9)-O(3)	1.152(6)

within 0.02 Å as is the C(1)C(6)C(5)C(4) unit. The dihedral angle between these two planes is 39.9° for (7) and 40.5° for (8), in the range found in other cyclohexadiene iron carbonyl structures.<sup>20,21</sup> The C-C bond lengths for the diene units are listed in Table 8, and the bond lengths

TABLE 7

Bond angles (°) for complex (8)

C(1)-Fe(1)-C(2)	38.9(2)	Fe(1)-C(1)-C(2)	69.9(3)
C(1)-Fe(1)-C(3)	70.0(2)	Fe(1)-C(1)-C(6)	109.5(4)
C(2)-Fe(1)-C(3)	39.5(2)	Fe(1)-C(2)-C(1)	71.2(3)
C(1)-Fe(1)-C(4)	75.8(2)	Fe(1)-C(2)-C(3)	68.6(3)
C(2)-Fe(1)-C(4)	68.3(2)	Fe(1)-C(3)-C(2)	71.8(3)
C(3)-Fe(1)-C(4)	40.2(2)	Fe(1)-C(3)-C(4)	71.0(3)
C(1)-Fe(1)-C(8)	89.5(3)	Fe(1)-C(4)-C(3)	68.8(3)
C(2)-Fe(1)-C(8)	128.1(2)	Fe(1)-C(4)-C(5)	110.3(3)
C(3)-Fe(1)-C(8)	138.0(2)	C(2)-C(1)-C(6)	118.9(5)
C(4)-Fe(1)-C(8)	100.5(2)	C(1)-C(2)-C(3)	116.7(5)
C(1)-Fe(1)-C(9)	95.8(2)	C(2)-C(3)-C(4)	112.3(5)
C(2)-Fe(1)-C(9)	89.5(2)	C(3)-C(4)-C(5)	121.6(5)
C(3)-Fe(1)-C(9)	113.8(2)	C(4)-C(5)-C(6)	110.0(4)
C(4)-Fe(1)-C(9)	153.9(2)	C(11)-P(1)-C(5)	110.6(5)
C(8)-Fe(1)-C(9)	104.1(3)	Fe(1)-C(2)-O(1)	126.3(3)
C(1)-Fe(1)-P(1)	167.6(1)	C(1)-C(2)-O(1)	118.1(4)
C(2)-Fe(1)-P(1)	132.1(2)	C(3)-C(2)-O(1)	124.9(5)
C(3)-Fe(1)-P(1)	98.2(1)	C(2)-O(1)-C(7)	116.4(5)
C(4)-Fe(1)-P(1)	93.0(1)	Fe(1)-C(8)-O(2)	176.1(5)
C(8)-Fe(1)-P(1)	97.7(2)	Fe(1)-C(9)-O(3)	176.6(5)
C(9)-Fe(1)-P(1)	92.2(2)	C(101)-P(1)-C(111)	100.3(2)
Fe(1)-P(1)-C(101)	118.5(1)	C(101)-P(1)-C(121)	103.3(1)
Fe(1)-P(1)-C(111)	116.1(1)	C(111)-P(1)-C(121)	103.4(2)
Fe(1)-P(1)-C(121)	113.1(1)	P(1)-C(111)-C(112)	117.1(1)
P(1)-C(101)-C(102)	120.4(1)	P(1)-C(111)-C(116)	122.8(1)
P(1)-C(101)-C(106)	119.6(1)	P(1)-C(121)-C(122)	117.4(1)
P(1)-C(121)-C(126)	122.1(1)		

and angles involving C(5) and C(6) indicate that they are  $sp^3$  hybridised. As in other complexes the Fe-C(2), C(3) bond lengths are slightly shorter than the Fe-C(1), C(4) distances so that the diene is tilted with respect to the metal.

The carbonyl ligands in both complexes are approximately linear, and the geometry of the triphenylphosphine ligands do not deviate significantly from the idealised values. The P(1)-Fe(1)-C(carbonyl) angles are narrower than the corresponding C(carbonyl)-Fe(1)-C(carbonyl) angles which may indicate that the steric effect of the phosphine ligand affects more its attitude relative to the diene rather than CO ligands. All the bond angles at iron involving the carbonyl and phosphine ligands are significantly less than the tetrahedral angle of 109.5° and some are closer to the value of 90.0°

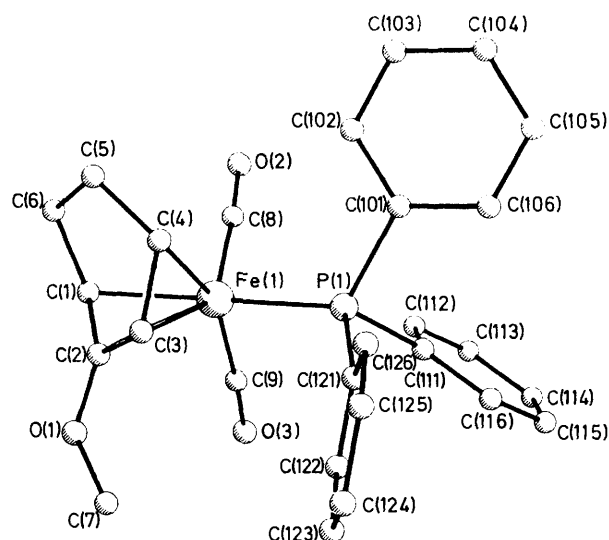
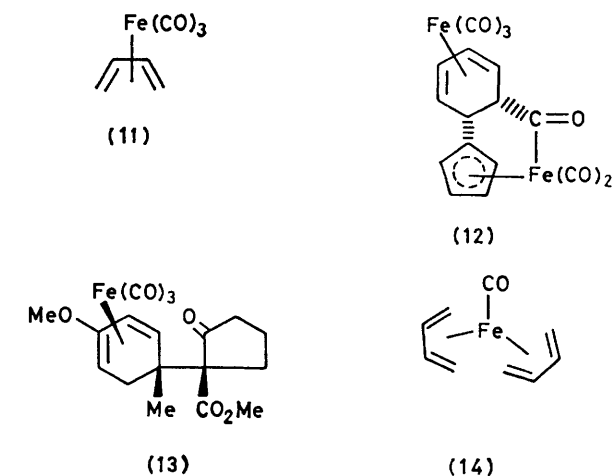


FIGURE 3 The molecular structure of (8)

TABLE 8  
Selected bond lengths (Å) for diene-Fe(CO)<sub>2</sub>L complexes



Complex	C(1,2)	C(2,3)	C(3,4)	C-O
(11) <sup>a</sup>	1.46	1.45	1.46	1.18, 1.13, 1.14
(12) <sup>b</sup>	1.43	1.39	1.43	1.15, 1.13, 1.13
(13) <sup>c</sup>	1.41	1.39	1.41	1.15, 1.14, 1.13
(7)	1.41	1.41	1.40	1.15, 1.14
(8)	1.41	1.41	1.43	1.16, 1.15
(14) <sup>d</sup>	1.43	1.46	1.43	1.02

<sup>a</sup> Ref. 23. <sup>b</sup> Ref. 24. <sup>c</sup> Ref. 21. <sup>d</sup> Ref. 22.

expected for octahedral co-ordination. It is perhaps better to consider the iron to have octahedral  $d^2sp^3$  hybridisation rather than that for tetrahedral co-ordination (see later).

**X-Ray Data.**—Table 8 summarises some of the relevant data for a number of diene-Fe(CO)<sub>3</sub> complexes from the literature and our own data for (7) and (8) (see above). In general for diene-Fe(CO)<sub>3</sub> complexes the central (2,3) bond is significantly shorter than the terminal (1,2 and 3,4) bonds. Complexes (7) and (8) show *approximately* equal lengths for diene C-C bonds, though clearly we cannot attach too much significance to the values. The variation in bond length *trans* to triphenylphosphine may well be due to crystal packing effects<sup>7</sup> and not an

effect of the methoxy-substituent since the same substituent in (13) does not lead to similar changes. An interesting result is the literature data for bis(butadiene)-monocarbonyliron (14) which now shows the terminal diene bonds rather shorter than the central bond.<sup>22</sup> It is likely that butadiene is a poorer  $\pi$  acceptor than CO, so that as far as these data go it is in complete agreement with the <sup>13</sup>C n.m.r. measurements. It may be noted that complexes (7) and (8) adopt similar conformations in the solid state (see below), and this in some ways limits the X-ray method, whereas the <sup>13</sup>C n.m.r. spectra for complexes (3), (5), and (7) were completely symmetrical, indicating their fluxional nature. (No change was observed down to -70 °C.) Thus, the n.m.r. method gives an average picture which randomises the effects of the ligands L. Furthermore, it is an exceedingly sensitive means of detecting relatively small electronic perturbations in an organometallic system, possibly superior to X-ray methods. It may also be noted that the C-O bond lengths of the carbonyl ligands are not appreciably changed, whereas it is readily accepted from i.r. data that the  $\pi$ -bond orders are considerably altered by ligand replacement.

**Interpretation of Results.**—A bonding model. Molecular-orbital calculations on butadiene-Fe(CO)<sub>3</sub> have

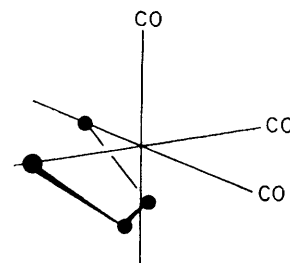


FIGURE 4 Arrangement of diene in octahedral environment of diene-Fe(CO)<sub>3</sub> complex

revealed that the iron  $d$  orbitals which are involved in  $\pi$  bonding to the CO ligands have an *antibonding* interaction with the diene.<sup>6</sup> On this basis we should expect that expansion of these orbitals, consequent upon replacing CO by a weaker  $\pi$  acceptor, will lead to increased anti-

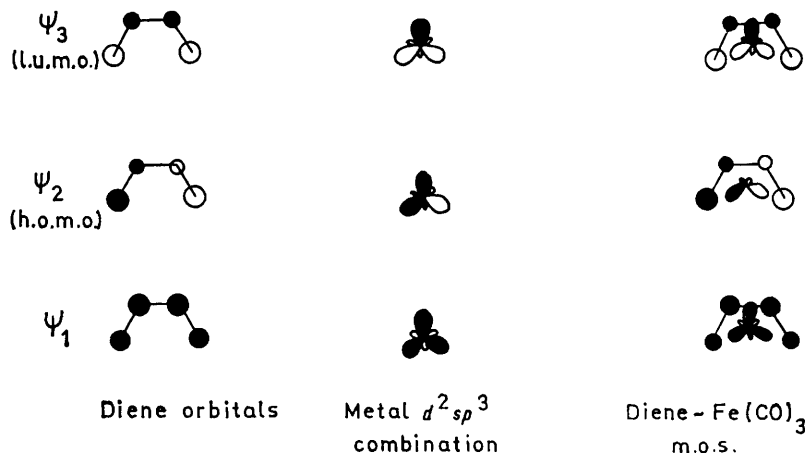


FIGURE 5 Orbital combinations for diene-Fe bonding

bonding interaction. The diene orbital populations would then show a small shift towards those of the uncomplexed state, and this now offers an explanation for the above observations. The available X-ray data<sup>7,21,23,24</sup> suggest a pseudo-octahedral symmetry for diene-Fe(CO)<sub>3</sub> complexes, indicated in Figure 4, in which primary orbital interactions occur between metal  $d^2sp^3$  hybrid orbitals and diene  $p$  orbitals, consistent with the calculations of Elian and Hoffmann<sup>5</sup> (Figure 5). We expect only a secondary interaction with the metal  $\pi$ -bonding orbitals. This suggests a delicate balance between  $\sigma$ -donor and  $\pi$ -acceptor effects, which may well account for the slightly anomalous triphenylphosphine result, owing to its steric requirement.<sup>25</sup>

We have not at this stage embarked upon a theoretical interpretation of the above effects, but hope that the pictorial model presented will form the basis for more detailed investigation.

(PPh<sub>3</sub>)<sub>2</sub> (1.7 g) was removed by filtration. The liquors were evaporated, cyclohexanol removed at 0.1 mmHg,\* and the residue was recrystallised from hexane to give dicarbonyl(cyclohexadiene)(triphenylphosphine)iron (7) (6.40 g, 62%) as a yellow crystalline solid, m.p. 120–121 °C;  $\delta$  (<sup>1</sup>H) (CDCl<sub>3</sub>): 7.6–7.2 (15 H, m, PPh<sub>3</sub>), 4.85 (2 H, m,  $J_{1,2}$  5,  $J_{2,4}$  3,  $J_{P,H}$  3.5 Hz, H<sup>2</sup> and H<sup>3</sup>), 2.52 (2 H, m, br, H<sup>1</sup> and H<sup>4</sup>), 1.9–1.2 (4 H, m, 2 × CH<sub>2</sub>) (Found: C, 68.5; H, 5.4. Calc. for C<sub>26</sub>H<sub>23</sub>FeO<sub>2</sub>P: C, 68.6; H, 5.1%).

Tricarbonyl(2-methoxycyclohexadiene)iron gave dicarbonyl(2-methoxycyclohexadiene)(triphenylphosphine)iron (15%), m.p. 159–160 °C;  $\delta$  (<sup>1</sup>H) (CDCl<sub>3</sub>): 7.7–7.2 (15 H, m, PPh<sub>3</sub>), 4.13 (1 H, ddd,  $J_{3,4}$  6,  $J_{1,3}$  2,  $J_{P,H}$  6 Hz, H<sup>3</sup>), 3.33 (3 H, s, OMe), 3.26 (1 H, m, H<sup>1</sup>), 1.9–1.2 (5 H, m, 2 × CH<sub>2</sub> and H<sup>4</sup>) (Found: C, 67.2; H, 5.3. Calc. for C<sub>27</sub>H<sub>25</sub>FeO<sub>3</sub>P: 66.9; H, 5.2%. *M* 484).

Butadiene(tricarbonyl)iron gave butadiene(dicarbonyl)(triphenylphosphine)iron (10) (40%), m.p. 144–145.5 °C;  $\delta$  (<sup>1</sup>H) (CDCl<sub>3</sub>): 7.9–7.1 (15 H, m, PPh<sub>3</sub>), 5.12 (2 H, m,  $J_{P,H}$

TABLE 9

Crystal and refinement data		
	Complex (7)	Complex (8)
Crystal habit	Hexagonal plate	Elongated rectangular block
Colour	Yellow	Pale yellow
Size (mm)	0.45 × 0.44 × 0.04	0.23 × 0.31 × 0.47
Molecular formula	C <sub>26</sub> H <sub>23</sub> FeO <sub>2</sub> P	C <sub>27</sub> H <sub>25</sub> FeO <sub>3</sub> P
Molecular weight	454.26	484.25
Crystal system	Monoclinic	Monoclinic
Space group	<i>P</i> 2 <sub>1</sub> / <i>c</i>	<i>P</i> 2 <sub>1</sub> / <i>c</i>
<i>a</i> (Å)	10.289(4)	14.444(7)
<i>b</i> (Å)	24.651(10)	18.052(10)
<i>c</i> (Å)	9.282(4)	9.229(4)
$\beta$ (°)	109.37(3)	100.57(4)
<i>U</i> (Å <sup>3</sup> )	2 221.0	2 365.6
<i>Z</i>	4	4
<i>D</i> <sub>c</sub> (g cm <sup>-3</sup> )	1.358	1.359
<i>D</i> <sub>m</sub> (g cm <sup>-3</sup> )	1.36	1.35
<i>F</i> (000)	943.96	995.96
$\mu$ (Mo- <i>K</i> $\alpha$ )(cm <sup>-1</sup> )	7.35	6.95
Number of intensities measured	5 034	4 366
2 $\theta$ Range for data collection	3.0 < 2 $\theta$ < 55.0°	3.0 < 2 $\theta$ < 55.0°
Number of significant intensities used in structure refinement	3 325	2 952
$\sigma$ Cut-off [ <i>F</i> > <i>n</i> $\sigma$ ( <i>F</i> )]	<i>n</i> = 3	<i>n</i> = 4
Weighting scheme	$[\sigma^2(F) + 0.0008 F_o ^2]^{-1}$	$[\sigma^2(F)]^{-1}$
Mean shift to error	0.005	0.020
<i>R</i>	0.053	0.062
<i>R</i> ' (= $\Sigma w^{\frac{1}{2}}\Delta/\Sigma w^{\frac{1}{2}} F_o $ )	0.052	0.055

## EXPERIMENTAL

Proton-decoupled, single-frequency off-resonance proton-decoupled, and gated-proton-decoupled, natural abundance <sup>13</sup>C n.m.r. spectra were measured on a JEOL FT-60 spectrometer operating at 15.1 MHz and 304 K, by the pulsed Fourier-transform method. Solutions in deuteriochloroform were prepared in the usual way.<sup>10,11</sup> Proton n.m.r. spectra were recorded on a Varian HA100 spectrometer and i.r. spectra on a Perkin-Elmer 577 instrument.

**Preparation of Complexes.**—The method is given for the triphenylphosphine complex (7). Other complexes were prepared in an identical fashion. Tricarbonyl(cyclohexadiene)iron (1) (5.0 g) and triphenylphosphine (6.0 g) were refluxed under nitrogen overnight in cyclohexanol. The mixture was cooled, light petroleum (b.p. 40–60 °C) (100 cm<sup>3</sup>) was added, and the resulting precipitate of [Fe(CO)<sub>3</sub>-

(PPh<sub>3</sub>)<sub>2</sub>] (1.7 g) was removed by filtration. The liquors were evaporated, cyclohexanol removed at 0.1 mmHg,\* and the residue was recrystallised from hexane to give dicarbonyl(cyclohexadiene)(triphenylphosphine)iron (7) (6.40 g, 62%) as a yellow crystalline solid, m.p. 120–121 °C;  $\delta$  (<sup>1</sup>H) (CDCl<sub>3</sub>): 7.6–7.2 (15 H, m, PPh<sub>3</sub>), 4.85 (2 H, m,  $J_{1,2}$  5,  $J_{2,4}$  3,  $J_{P,H}$  3.5 Hz, H<sup>2</sup> and H<sup>3</sup>), 2.52 (2 H, m, br, H<sup>1</sup> and H<sup>4</sup>), 1.9–1.2 (4 H, m, 2 × CH<sub>2</sub>) (Found: C, 68.5; H, 5.4. Calc. for C<sub>26</sub>H<sub>23</sub>FeO<sub>2</sub>P: C, 68.6; H, 5.1%).

Tricarbonyl(cyclohexadiene)iron with triphenylarsine gave dicarbonyl(cyclohexadiene)(triphenylarsine)iron (5) (40%), m.p. 104–106 °C;  $\delta$  (<sup>1</sup>H) (CDCl<sub>3</sub>): 7.6–7.1 (15 H, AsPh<sub>3</sub>), 5.0 (2 H, dd, *J* 5, 2 Hz, H<sup>2</sup>, H<sup>3</sup>), 2.60 (2 H, m, br, H<sup>1</sup>, H<sup>4</sup>), 1.8–1.2 (4 H, m, 2 × CH<sub>2</sub>) (Found: C, 62.6; H, 4.8. Calc. for C<sub>26</sub>H<sub>23</sub>AsFeO<sub>2</sub>: C, 62.7; H, 4.7%).

Tricarbonyl(2-methoxycyclohexadiene)iron with triphenylarsine gave dicarbonyl(2-methoxycyclohexadiene)(triphenylarsine)iron (6) (10%), m.p. 146–148 °C;  $\delta$  (<sup>1</sup>H) (CDCl<sub>3</sub>): 7.5–7.2 (15 H, AsPh<sub>3</sub>), 4.50 (1 H, dd, *J* 6, 2 Hz, H<sup>3</sup>), 3.25 (3 H, s, OMe), 3.10 (1 H, m, H<sup>1</sup>), 2.0 (1 H, m, H<sup>4</sup>), 1.70–1.30 (4 H, m, 2 × CH<sub>2</sub>) (Found: C, 61.3; H, 5.1. Calc. for C<sub>27</sub>H<sub>25</sub>AsFeO<sub>3</sub>: C, 61.4; H, 4.8%).

Tricarbonyl(cyclohexadiene)iron with trimethyl phosphite gave dicarbonyl(cyclohexadiene)(trimethyl phosphite)iron (3) (20%) obtained as a yellow oil after preparative-layer

\* Throughout this paper: 1 mmHg  $\approx$  13.6 × 9.8 Pa.

chromatography.  $\delta$  ( $^1\text{H}$ ) ( $\text{CDCl}_3$ ): 4.98 (2 H, m,  $\text{H}^2$ ,  $\text{H}^3$ ), 3.48 [9 H, d,  $J_{\text{P,H}}$  12 Hz,  $\text{P}(\text{OMe})_3$ ], 2.92 (2 H, m, br,  $\text{H}^1$ ,  $\text{H}^4$ ), 1.9—1.4 (4 H, m,  $2 \times \text{CH}_2$ ) (Found: C, 41.8; H, 5.5. Calc. for  $\text{C}_{11}\text{H}_{17}\text{FeO}_5\text{P}$ : C, 41.8; H, 5.4%).

*Tricarbonyl(2-methoxycyclohexadiene)iron* with trimethyl phosphite gave dicarbonyl(2-methoxycyclohexadiene)(trimethyl phosphite)iron (4) (10%) as a yellow oil after preparative-layer chromatography.  $\delta$  ( $^1\text{H}$ ) ( $\text{CDCl}_3$ ): 4.80 (1 H, m,  $\text{H}^3$ ), 3.58 (3 H, s, OMe), 3.54 [9 H, d,  $J_{\text{P,H}}$  8 Hz,  $\text{P}(\text{OMe})_3$ ], 3.24 (1 H, m,  $\text{H}^1$ ), 2.40 (1 H, m,  $\text{H}^4$ ), 1.8—1.1 (4 H,  $2 \times \text{CH}_2$ ) (Found: C, 41.9; H, 5.3. Calc. for  $\text{C}_{12}\text{H}_{19}\text{FeO}_6\text{P}$ : C, 41.6; H, 5.5%).

TABLE 10

Atom co-ordinates ( $\times 10^4$ ) for complex (7)

Atom	$x/a$	$y/b$	$z/c$
Fe(1)	5 360(1)	1 657(1)	884(1)
C(1)	3 598(4)	2 117(2)	-248(5)
C(2)	4 300(4)	1 956(2)	-1 245(5)
C(3)	4 485(4)	1 390(3)	-1 327(5)
C(4)	3 936(4)	1 077(2)	-402(5)
C(5)	2 515(4)	1 202(2)	-320(6)
C(6)	2 303(4)	1 810(2)	-245(6)
C(7)	4 924(4)	1 605(2)	2 550(5)
O(7)	4 587(4)	1 579(1)	3 613(4)
C(8)	6 460(4)	2 230(2)	1 292(5)
O(8)	7 138(4)	2 608(1)	1 550(5)
P(1)	7 152(1)	1 090(1)	1 522(1)
C(9)	8 750(4)	1 384(2)	2 843(4)
C(10)	9 998(4)	1 381(2)	2 597(5)
C(11)	11 151(4)	1 619(2)	3 663(6)
C(12)	11 062(5)	1 855(2)	4 956(5)
C(13)	9 816(5)	1 869(2)	5 206(5)
C(14)	8 660(4)	1 634(2)	4 150(5)
C(15)	7 679(4)	856(2)	-77(4)
C(16)	7 805(4)	319(2)	-420(5)
C(17)	8 156(5)	184(2)	-1 715(5)
C(18)	8 376(5)	578(2)	-2 628(5)
C(19)	8 264(5)	1 117(2)	-2 291(6)
C(20)	7 911(5)	1 254(2)	-1 029(5)
C(21)	7 055(4)	462(1)	2 554(4)
C(22)	5 820(4)	307(2)	2 751(5)
C(23)	5 767(5)	-164(2)	3 564(5)
C(24)	6 920(5)	-481(2)	4 176(5)
C(25)	8 156(5)	-327(2)	3 988(5)
C(26)	8 218(4)	136(2)	3 191(4)

TABLE 11

Hydrogen-atom co-ordinates ( $\times 10^4$ ) and isotropic thermal parameters ( $10^3 \times \text{\AA}^2$ ) for complex (7)

Atom	$x/a$	$y/b$	$z/c$	$U$
H(1)	3 228(4)	2 519(2)	-112(5)	96(7)
H(2)	4 669(4)	2 242(2)	-1 900(5)	70(3)
H(3)	5 009(4)	1 211(2)	-2 045(5)	70(3)
H(4)	3 838(4)	640(2)	-405(5)	96(7)
H(51)	2 413(4)	1 014(2)	689(6)	96(7)
H(52)	1 742(4)	1 041(2)	-1 322(6)	96(7)
H(61)	1 443(4)	1 934(2)	-1 223(6)	96(7)
H(62)	2 087(4)	1 905(2)	789(6)	96(7)
H(10)	10 085(4)	1 195(2)	1 579(5)	70(3)
H(11)	12 125(4)	1 616(2)	3 460(6)	70(3)
H(12)	11 966(5)	2 031(2)	5 780(5)	70(3)
H(13)	9 737(5)	2 061(2)	6 219(5)	70(3)
H(14)	7 683(4)	1 647(2)	4 357(5)	70(3)
H(16)	7 635(4)	3(2)	303(5)	70(3)
H(17)	8 250(5)	237(2)	-1 986(5)	70(3)
H(18)	8 640(5)	469(2)	-3 624(5)	70(3)
H(19)	8 452(5)	1 430(2)	-3 011(6)	70(3)
H(20)	7 812(5)	1 676(2)	-774(5)	70(3)
H(22)	4 907(4)	552(2)	2 277(5)	70(3)
H(23)	4 808(5)	-282(2)	3 713(5)	70(3)
H(24)	6 867(5)	-845(2)	4 798(5)	70(3)
H(25)	9 067(5)	-573(2)	4 469(5)	70(3)
H(26)	9 183(4)	251(2)	3 053(4)	70(3)

TABLE 12

Atom co-ordinates ( $\times 10^4$ ) for complex (8)

Atom	$x/a$	$y/b$	$z/c$
Fe(1)	2 189(1)	5 703(1)	3 344(1)
C(1)	2 088(4)	6 865(3)	3 624(7)
C(2)	2 074(3)	6 500(3)	4 976(6)
C(3)	2 815(3)	5 999(3)	5 457(6)
C(4)	3 508(3)	6 005(3)	4 538(6)
C(5)	3 837(4)	6 723(3)	3 938(7)
C(6)	2 987(4)	7 228(3)	3 389(7)
O(1)	1 314(3)	6 607(2)	5 633(5)
C(7)	1 197(5)	6 083(4)	6 780(8)
C(8)	2 366(4)	5 849(3)	1 551(6)
O(2)	2 487(3)	5 989(3)	371(5)
C(9)	967(4)	5 528(3)	3 141(6)
O(3)	167(3)	5 445(2)	3 046(5)
P(1)	2 531(1)	4 501(1)	3 488(2)
C(101)	3 564(2)	4 171(1)	2 742(4)
C(102)	4 181(2)	4 676(1)	2 280(4)
C(103)	4 953(2)	4 422(1)	1 710(4)
C(104)	5 109(2)	3 663(1)	1 602(4)
C(105)	4 492(2)	3 158(1)	2 064(4)
C(106)	3 720(2)	3 411(1)	2 634(4)
C(111)	1 615(2)	3 871(1)	2 527(4)
C(112)	1 114(2)	4 104(1)	1 165(4)
C(113)	442(2)	3 640(1)	349(4)
C(114)	269(2)	2 943(1)	895(4)
C(115)	770(2)	2 710(1)	2 257(4)
C(116)	1 442(2)	3 174(1)	3 073(4)
C(121)	2 754(2)	4 150(2)	5 379(3)
C(122)	2 000(2)	4 148(2)	6 132(3)
C(123)	2 152(2)	3 979(2)	7 632(3)
C(124)	3 057(2)	3 811(2)	8 378(3)
C(125)	3 811(2)	3 813(2)	7 625(3)
C(126)	3 659(2)	3 983(2)	6 126(3)

TABLE 13

Hydrogen-atom co-ordinates ( $\times 10^4$ ) and isotropic thermal parameters ( $10^3 \times \text{\AA}^2$ ) for complex (8)

Atom	$x/a$	$y/b$	$z/c$	$U$
H(1)	1 465(4)	6 885(3)	2 776(7)	98(5)
H(3)	2 853(3)	5 650(3)	6 417(6)	98(5)
H(4)	3 807(3)	5 487(3)	4 262(6)	98(5)
H(51)	4 318(4)	7 002(3)	4 800(7)	78(8)
H(52)	4 192(4)	6 600(3)	3 033(7)	78(8)
H(61)	2 946(4)	7 336(3)	2 228(7)	78(8)
H(62)	3 078(4)	7 744(3)	3 990(7)	78(8)
H(71)	593(5)	6 211(4)	7 273(8)	214(19)
H(72)	1 827(5)	6 095(4)	7 618(8)	214(19)
H(73)	1 113(5)	5 538(4)	6 291(8)	214(19)
H(102)	4 060(2)	5 263(1)	2 364(4)	98(5)
H(103)	5 430(2)	4 813(1)	1 352(4)	98(5)
H(104)	5 706(2)	3 467(1)	1 160(4)	98(5)
H(105)	4 613(2)	2 570(1)	1 980(4)	98(5)
H(106)	3 243(2)	3 020(1)	2 992(4)	98(5)
H(112)	1 248(2)	4 644(1)	742(4)	98(5)
H(113)	54(2)	3 820(1)	-705(4)	98(5)
H(114)	-252(2)	2 583(1)	263(4)	98(5)
H(115)	636(2)	2 170(1)	2 679(4)	98(5)
H(116)	1 830(2)	2 994(1)	4 127(4)	98(5)
H(122)	1 299(2)	4 278(2)	5 554(3)	98(5)
H(123)	1 568(2)	3 977(2)	8 215(3)	98(5)
H(124)	3 175(2)	3 680(2)	9 539(3)	98(5)
H(125)	4 512(2)	3 683(2)	8 203(3)	98(5)
H(126)	4 243(2)	3 984(2)	5 542(3)	98(5)

*X-Ray Structural Analyses of (7) and (8).*—Crystals of (7) and (8) were mounted in 0.5-mm Lindemann tubes under a nitrogen atmosphere. Cell dimensions and space groups were determined from preliminary Weissenberg photographs. The two data sets were recorded on a Syntex  $P2_1$  four-circle diffractometer using graphite-monochromated Mo- $K_\alpha$  radiation ( $\lambda_{\text{M1}}$  0.709 26,  $\lambda_{\text{M2}}$  0.713 54 Å) and a 96-step  $\omega$ -2 $\theta$  scan procedure; peaks were scanned from 1.0°

below  $K_{\alpha 1}$  to  $1.0^\circ$  above  $K_{\alpha 2}$  at rates between 0.033 33 and  $0.4883^\circ \text{ s}^{-1}$ , dependent on an initial 2-s peak count; reflections with intensities of  $\leq 8 \text{ counts s}^{-1}$  were not remeasured. For both data collections two check reflections were monitored periodically but showed no significant variations. For the two complexes accurate cell parameters were obtained from the angular measurements of 15 strong reflections in the range  $20 < 2\theta < 30.0^\circ$ . Details of the data collection and structure refinement are given in Table 9.

In both structures the Fe atoms were located from Patterson syntheses, and the remaining non-hydrogen atoms from subsequent Fourier-difference maps. All atoms were assigned isotropic temperature factors, and after several cycles of refinement, further electron-density difference maps revealed the positions of most of the hydrogen atoms. All hydrogen atoms were placed in idealised positions and constrained to ride  $1.08 \text{ \AA}$  from the relevant carbon atom, and each type of H atom was assigned a common isotropic temperature factor; the methyl and phenyl groups in (8) were refined as rigid bodies. All the non-hydrogen atoms in (7) were assigned anisotropic thermal parameters, and all those apart from the phenyl carbons in (8). Refinement continued by blocked-cascade least squares until convergence was reached. Final Fourier-difference maps revealed no significant regions of electron density.

Complex neutral-atom scattering factors were employed.<sup>26</sup> All computations were performed on the University of Cambridge IBM370/165 computer using programs written by Professor G. M. Sheldrick. The molecular diagrams were drawn using the 'PLUTO' plotting program written by Dr. W. D. S. Motherwell. The atomic fractional co-ordinates of the non-hydrogen and hydrogen atoms for (7) are given in Tables 10 and 11 respectively, and the corresponding data for (8) in Tables 12 and 13. Details of thermal parameters, bond angles involving hydrogen atoms, observed and calculated structure factors, and of least-squares planes for the two compounds have been deposited as Supplementary Publication No. SUP 22989 (45 pp).\*

We are grateful to the S.R.C. for financial support.

[0/1218 Received, 1st August, 1980]

\* For details see Notices to Authors No. 7, *J. Chem. Soc., Dalton Trans.*, 1979, Index issue.

## REFERENCES

- <sup>1</sup> I. Fleming, 'Frontier Orbitals and Organic Chemical Reactions,' Wiley, London, 1976, and refs. therein.
- <sup>2</sup> J. Chatt and L. A. Duncanson, *J. Chem. Soc.*, 1953, 2039; M. J. S. Dewar, *Bull. Soc. Chim. Fr.*, 1951, 18, C71.
- <sup>3</sup> G. E. Coates, M. L. H. Green, and K. Wade, 'Organometallic Compounds,' vol. 2, 'The Transition Elements,' 3rd. edn., Chapman and Hall, London, 1972.
- <sup>4</sup> D. M. P. Mingos, *J. Chem. Soc., Dalton Trans.*, 1977, 20; 28; 31.
- <sup>5</sup> M. Elian and R. Hoffmann, *Inorg. Chem.*, 1975, 14, 1058.
- <sup>6</sup> J. A. Connor, L. M. R. Derrick, M. B. Hall, I. H. Hillier, M. F. Guest, B. R. Higginson, and D. R. Lloyd, *Mol. Phys.*, 1974, 28, 1193.
- <sup>7</sup> C. Kruger, B. L. Barnett, and D. Brauer, 'The Organic Chemistry of Iron,' eds. E. A. Koerner von Gustorf, F. W. Grevels, and I. Fischler, Academic Press, New York, 1978, ch. 1, and refs. therein.
- <sup>8</sup> A. Almenningen, O. Bastiensen, and M. Traetteberg, *Acta Chem. Scand.*, 1958, 12, 1221.
- <sup>9</sup> M. Azzaro, J. F. Gal, S. Géribaldi, and N. Novo-Kremer, *Org. Magn. Reson.*, 1977, 9, 181, and refs. therein.
- <sup>10</sup> A. J. Pearson, *Aust. J. Chem.*, 1976, 29, 1679.
- <sup>11</sup> A. J. Pearson, *Aust. J. Chem.*, 1977, 30, 407.
- <sup>12</sup> F. A. Cotton and G. Wilkinson, 'Advanced Inorganic Chemistry,' 2nd edn., Wiley Interscience, New York, 1966, p. 746.
- <sup>13</sup> M. R. Churchill and R. Mason, *Adv. Organomet. Chem.*, 1967, 5, 93.
- <sup>14</sup> B. F. Hallam and P. L. Pauson, *J. Chem. Soc.*, 1958, 642.
- <sup>15</sup> L. J. Bellamy, 'The Infrared Spectra of Complex Molecules,' 3rd edn., Chapman and Hall, London, 1975.
- <sup>16</sup> A. J. Pearson, *J. Chem. Soc., Perkin Trans. 1*, 1979, 1255; A. J. Birch and K. P. Dastur, *ibid.*, 1973, 1650.
- <sup>17</sup> G. R. Stephenson, Ph.D. Thesis, University of Cambridge, 1978.
- <sup>18</sup> J. A. Pople, W. G. Schneider, and H. J. Bernstein, 'High Resolution Nuclear Magnetic Resonance,' McGraw-Hill, New York, 1959, ch. 8.
- <sup>19</sup> K. N. Houk, *J. Am. Chem. Soc.*, 1973, 95, 4092; K. N. Houk, J. Sims, R. E. Duke, jun., R. W. Strozier, and J. K. George, *ibid.*, 1973, 95, 7287.
- <sup>20</sup> F. A. Cotton and J. M. Troup, *J. Organomet. Chem.*, 1974, 77, 369; J. J. Guy, B. E. Reichert, and G. M. Sheldrick, *Acta Crystallogr., Sect. B*, 1976, 32, 2504; B. F. G. Johnson, J. Lewis, D. G. Parker, P. R. Raithby, and G. M. Sheldrick, *J. Organomet. Chem.*, 1978, 150, 115.
- <sup>21</sup> A. J. Pearson and P. R. Raithby, *J. Chem. Soc., Perkin Trans. 1*, 1980, 395.
- <sup>22</sup> D. A. Whiting, *Cryst. Struct. Commun.*, 1972, 1, 379.
- <sup>23</sup> O. S. Mills and G. Robinson, *Proc. Chem. Soc.*, 1960, 421; *Acta Crystallogr.*, 1963, 16, 758.
- <sup>24</sup> M. R. Churchill and S. W.-Y. Chang, *Inorg. Chem.*, 1977, 129, 105.
- <sup>25</sup> C. A. Tolman, *Chem. Rev.*, 1977, 77, 313.
- <sup>26</sup> 'International Tables for X-Ray Crystallography,' Kynoch Press, Birmingham, 1974, vol. 4.